Proceedings of 20th International Congress on Acoustics, ICA 2010

23–27 August 2010, Sydney, Australia

Active noise control at a virtual acoustic energy density sensor in a three-dimensional sound field

D.J. Moreau, B.S. Cazzolato and A.C. Zander

School of Mechanical Engineering, The University of Adelaide, Adelaide, SA, 5005 Australia

PACS: 43.50.Ki

ABSTRACT

A common problem in local active noise control is that the zone of quiet centered at the physical microphone is too small to extend to the desired location of attenuation, such as an observer's ear. The physical microphone must therefore be placed at the desired location of attenuation, which is often inconvenient. Virtual microphones overcome this by shifting the zone of quiet away from the physical microphone to a desired location of attenuation, referred to as the virtual location. In an effort to extend the zone of quiet generated at the virtual location, a virtual acoustic energy density method is developed in this paper for use in a three-dimensional sound field. This virtual energy density method uses a modified version of the remote microphone technique to estimate the total acoustic energy density at a virtual location. Experimental results of active noise control at a virtual acoustic energy density sensor and a virtual microphone in a three-dimensional sound field are presented for comparison. Minimising the total virtual acoustic energy density with the active noise control system is shown to create a spatially extended zone of quiet at a fixed virtual location compared to virtual pressure control.

INTRODUCTION

A traditional local active noise control system creates a zone of quiet at a physical microphone by minimising the measured acoustic sound pressure with a single secondary sound source. While noise levels are significantly attenuated at the microphone location, the zone of quiet is generally small and impractically sized. Elliott et al. (1988) demonstrated both analytically and experimentally that the zone of quiet generated at a microphone in a pure tone diffuse sound field is defined by a *sinc* function, with the primary sound pressure level reduced by 10 dB over a sphere of diameter one tenth of the excitation wavelength, $\lambda/10$. In addition to the zone of quiet being small, the sound pressure levels outside of the zone of quiet are likely to be higher than the original disturbance alone. This is shown in Fig. 1 (a), where the zone of quiet located at the physical microphone is too small to extend to the observer's ear and the observer in fact experiences an increase in the sound pressure level with the active noise control system operating.

The zone of quiet generated at the physical sensor location may be enlarged by minimising the acoustic energy density instead of the acoustic sound pressure. Elliott and Garcia-Bonito (1995) investigated the control of both pressure and pressure gradient (equivalent to one-dimensional acoustic energy density (Nelson and Elliott 1992)) in a diffuse sound field with two secondary sources. Minimising both the pressure and pressure gradient along a single axis produced a 10 dB zone of quiet over a distance of $\lambda/2$, in the direction of pressure gradient measurement. This is considerably larger than the zone of quiet obtained by minimising pressure alone.

Virtual microphones are used in active noise control to shift the zone of quiet away from the physical microphone to a desired location of attenuation. This is shown in Fig. 1 (b), where the zone of quiet is shifted from the physical microphone to a virtual microphone located at the observer's ear. Using the physical error signal, a virtual sensing algorithm is used to estimate the pressure at the virtual location. Instead of minimising the physical error signal, the estimated pressure is minimised with the active noise control system to generate a zone of quiet at the virtual location. A number of virtual sensing algorithms have been developed in the past to estimate the pressure at a fixed virtual location including *the virtual microphone arrangement* (Elliott and David 1992), *the remote microphone technique* (Roure and Albarrazin 1999), *the forward difference prediction technique* (Cazzolato 1999), *the adaptive LMS virtual microphone technique* (Cazzolato 2002), *the Kalman filtering virtual sensing technique* (Petersen et al. 2008) and *the Stochastically Optimal Tonal Diffuse Field (SOTDF) virtual sensing method* (Moreau et al. 2009b).

In an effort to extend the localised zone of quiet generated at a fixed virtual location, one-dimensional virtual acoustic energy density sensors have been developed using the forward difference prediction technique (Kestell et al. 2000) and the SOTDF virtual sensing method (Moreau et al. 2009b). These one-dimensional virtual acoustic energy density sensors estimate the sound pressure and the pressure gradient along one of the three orthogonal axes. Forward difference prediction virtual energy density sensors were shown to produce a broader region of control compared to virtual microphones in numerical simulations and experiments conducted in a free field and a long narrow duct (Kestell et al. 2001a, Kestell 2000, Kestell et al. 2000; 2001b). Active noise control at a stochastically optimal virtual energy density sensor with two secondary sources in a pure tone diffuse sound field generates a zone of quiet with a diameter of approximately $\lambda/2$ at the virtual location (Moreau et al. 2009b). This is a five fold increase in the size of the zone of quiet compared to that obtained by cancelling the pressure at a virtual location alone.

In many applications, the virtual location is not spatially fixed. This occurs, for example, when the desired location of attenuation is the ear of a seated observer and the observer moves their head, thereby moving the virtual location. As a result, a number of moving virtual sensing algorithms have been developed

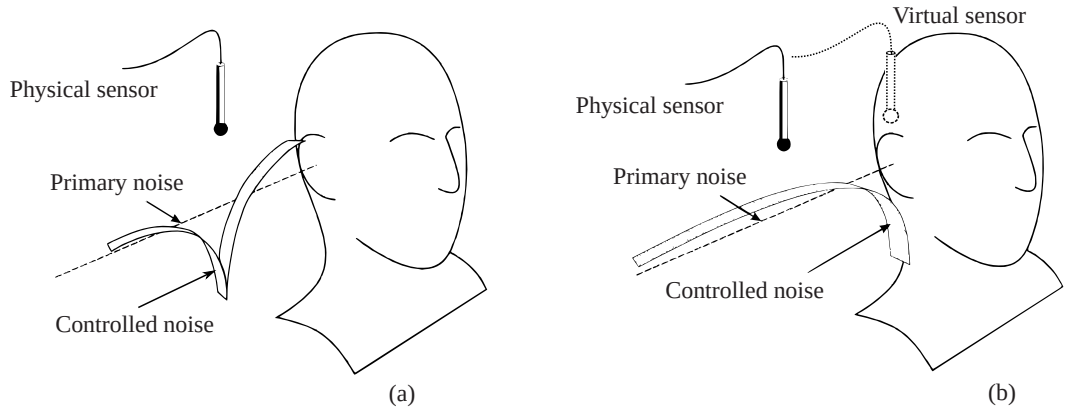

Figure 1: Comparison of local active noise control (a) at a physical sensor and (b) at a virtual sensor.

to generate a virtual microphone capable of tracking a moving virtual location including *the remote moving microphone technique* (Petersen et al. 2006), *the adaptive LMS moving virtual microphone technique* (Petersen et al. 2005), *the Kalman filtering moving virtual microphone technique* (Petersen 2007) and *the Stochastically Optimal Tonal Diffuse Field (SOTDF) moving virtual sensing method* (Moreau et al. 2009a). The performance of these moving virtual microphones has been experimentally investigated in an acoustic duct and at the ear of a rotating artificial head in a three-dimensional sound field. Results of real-time experimental control demonstrated that minimising the moving virtual error signal achieved greater attenuation at the moving virtual location than minimising the error signal at either a fixed physical or virtual microphone.

In this paper, a fixed three-dimensional virtual acoustic energy density sensing method is presented for use in a modally dense three-dimensional sound field. This virtual energy density method uses a modified version of the remote microphone technique (Roure and Albarrazin 1999) to estimate the sound pressure and the pressure gradient along all three of the orthogonal axes at a fixed virtual location. Experimental results of active noise control at a three-dimensional virtual energy density sensor and a virtual microphone are presented to compare the size of the localised zone of quiet achieved by minimising either the acoustic energy density or the squared pressure respectively. Four secondary sources are required in local acoustic energy density control to independently drive the pressure and the pressure gradients along the three orthogonal axes to zero. If only a single secondary source is used per energy density sensor there will be a trade off between the attenuation achieved at the error sensor location and the size of the localised zone of quiet.

The purpose of this study is to determine whether fixed virtual energy density sensors provide an alternative to moving virtual microphones. Moving virtual microphones create a moving zone of quiet capable of tracking an observer's ears during head rotations. As a seated observer moves their head through a relatively small region of the sound field, the spatially extended zone of quiet generated at a three-dimensional virtual acoustic energy density sensor may be large enough to encompass the path of the observer's ear. Minimising the acoustic energy density at a fixed virtual location may therefore be an alternative to active noise control at a moving virtual microphone.

The performance of one-dimensional virtual acoustic energy density sensors in local active noise control has been previously investigated in a free field and a long narrow duct using the forward difference prediction technique (Kestell et al. 2001a, Kestell 2000, Kestell et al. 2000; 2001b) and in a pure tone diffuse sound field using the SOTDF virtual sensing method (Moreau et al. 2009b). In many real would applications, however, it is likely that the sound field is neither perfectly free field nor perfectly diffuse. In this paper, the performance of three-dimensional virtual acoustic energy density sensors is experimentally investigated in a modally dense three-dimensional sound field. The experimental results presented here therefore demonstrate the performance of virtual acoustic energy density sensors in a sound field that is more likely to be encountered in practice.

THEORY

The remote energy density technique uses a modified version of the remote microphone technique (Roure and Albarrazin 1999) to generate a virtual energy density sensor at a spatially fixed virtual location. The total instantaneous acoustic energy density at a virtual location is given by

$$E_{D,v}(n) = \frac{1}{2}\rho \sum_{m=1}^{3} v_{v,m}^2(n) + \frac{p_v^2(n)}{2\rho c^2}, \qquad (1)$$

where $m = 1,2,3$ corresponds to the x, y and z direction respectively, $v_{v,m}(n)$ is the total particle velocity at the virtual location in the mth direction, $p_v(n)$ is the total sound pressure at the virtual location, ρ is the ambient fluid density, c is the speed of sound and n is the time step. The remote energy density technique estimates the acoustic sound pressure, $\tilde{p}_v(n)$, and the three components of particle velocity, $\tilde{v}_{v,1}(n)$, $\tilde{v}_{v,2}(n)$, and $\tilde{v}_{v,3}(n)$, at the virtual location. The total acoustic energy density at the virtual location is then calculated using Eq. 1. In the following description of the remote energy density technique, estimation of the sound pressure, $\tilde{p}_v(n)$, and the general mth component of particle velocity, $\tilde{v}_{v,m}(n)$, at the virtual location is derived for simplicity. In practice, all three components of particle velocity, $\tilde{v}_{v,1}(n)$, $\tilde{v}_{v,2}(n)$, and $\tilde{v}_{v,3}(n)$, must be calculated to obtain an estimate of the three-dimensional acoustic energy density.

The remote energy density technique calculates the acoustic pressure, $\tilde{p}_v(n)$, and the mth component of particle velocity, $\tilde{v}_{v,m}(n)$, at the virtual location using the acoustic pressure, $p_a(n)$, and the mth component of particle velocity, $v_{a,m}(n)$, measured with a physical energy density sensor. The remote energy density technique requires a preliminary identification stage in which a second acoustic energy density sensor is temporarily located at the virtual location. During the preliminary identification stage, the secondary transfer functions between the L secondary sources and each of the physical and virtual quantities, $p_a(n)$, $v_{a,m}(n)$, $p_v(n)$ and $v_{v,m}(n)$, are measured as vectors $\tilde{\mathbf{Z}}_{sa,p}$, $\tilde{\mathbf{Z}}_{sa,vm}$, $\tilde{\mathbf{Z}}_{sv,p}$ and $\tilde{\mathbf{Z}}_{sv,vm}$ respectively. The pri-

mary transfer functions between the pressure at the physical and virtual locations, $\tilde{M}_p$, and the particle velocity at the physical and virtual locations, $\tilde{M}_{v,m}$, are also estimated during this preliminary identification stage. The vectors of the secondary physical transfer functions, $\tilde{\mathbf{Z}}_{sa,p}$ and $\tilde{\mathbf{Z}}_{sa,vm}$, each of length L, are given by

$$\tilde{\mathbf{Z}}_{sa,p} = \left[\begin{array}{cccc} \tilde{Z}_{s1a,p} & \tilde{Z}_{s2a,p} & \dots & \tilde{Z}_{sLa,p} \end{array} \right], \quad (2)$$

$$\tilde{\mathbf{Z}}_{sa,vm} = \left[\begin{array}{cccc} \tilde{Z}_{s1a,vm} & \tilde{Z}_{s2a,vm} & \dots & \tilde{Z}_{sLa,vm} \end{array} \right], \quad (3)$$

where $\tilde{Z}_{sla,p}$ is the secondary transfer function between the lth secondary source and the pressure at the physical location, and $\tilde{Z}_{sla,vm}$ is the secondary transfer function between the lth secondary source and the mth component of the particle velocity at the physical location. The vectors of the secondary virtual transfer functions, $\tilde{\mathbf{Z}}_{sv,p}$ and $\tilde{\mathbf{Z}}_{sv,vm}$, each of length L, are similarly defined as

$$\tilde{\mathbf{Z}}_{sv,p} = \left[\begin{array}{cccc} \tilde{Z}_{s1v,p} & \tilde{Z}_{s2v,p} & \dots & \tilde{Z}_{sLv,p} \end{array} \right], \quad (4)$$

$$\tilde{\mathbf{Z}}_{sv,vm} = \left[\begin{array}{cccc} \tilde{Z}_{s1v,vm} & \tilde{Z}_{s2v,vm} & \dots & \tilde{Z}_{sLv,vm} \end{array} \right], \quad (5)$$

where $\tilde{Z}_{slv,p}$ is the secondary transfer function between the lth secondary source and the pressure at the virtual location, and $\tilde{Z}_{slv,vm}$ is the secondary transfer function between the lth secondary source and the mth component of the particle velocity at the virtual location.

A block diagram of the remote energy density technique is given in Fig. 2. As shown in Fig. 2, estimates of the primary pressure and the mth component of the primary particle velocity, $\tilde{p}_{pa}(n)$ and $\tilde{v}_{pa,m}(n)$, at the physical location are first calculated using

$$\tilde{p}_{pa}(n) = p_a(n) - \tilde{p}_{sa}(n) = p_a(n) - \tilde{\mathbf{Z}}_{sa,p}\mathbf{u}_s(n), \quad (6)$$

$$\tilde{v}_{pa,m}(n) = v_{a,m}(n) - \tilde{v}_{sa,m}(n) = v_{a,m}(n) - \tilde{\mathbf{Z}}_{sa,vm}\mathbf{u}_s(n), \quad (7)$$

where $\tilde{p}_{sa}(n)$ is an estimate of the secondary pressure at the physical location, $\tilde{v}_{sa,m}(n)$ is an estimate of the mth component of the secondary particle velocity at the physical location, and the strength of the L secondary sources is given by

$$\mathbf{u}_s(n) = \left[\begin{array}{cccc} u_{s1}(n) & u_{s2}(n) & \dots & u_{sL}(n) \end{array} \right]^{\mathrm{T}}. \quad (8)$$

Next, estimates of the primary pressure and the mth component of the primary particle velocity, $\tilde{p}_{pv}(n)$ and $\tilde{v}_{pv,m}(n)$, at the virtual location are obtained using

$$\tilde{p}_{pv}(n) = \tilde{M}_p\tilde{p}_{pa}(n), \quad (9)$$

$$\tilde{v}_{pv,m}(n) = \tilde{M}_{v,m}\tilde{v}_{pa,m}(n). \quad (10)$$

Finally, estimates, $\tilde{p}_v(n)$ and $\tilde{v}_{v,m}(n)$, of the total pressure and the mth component of the total particle velocity at the virtual location are calculated as

$$\tilde{p}_v(n) = \tilde{p}_{pv}(n) + \tilde{p}_{sv}(n) = \tilde{M}_p\tilde{p}_{pa} + \tilde{\mathbf{Z}}_{sv,p}\mathbf{u}_s(n), \quad (11)$$

$$\tilde{v}_{v,m}(n) = \tilde{v}_{pv,m}(n) + \tilde{v}_{sv,m}(n) = \tilde{M}_{v,m}\tilde{v}_{pa,m} + \tilde{\mathbf{Z}}_{sv,vm}\mathbf{u}_s(n), \quad (12)$$

where $\tilde{p}_{sv}(n)$ is an estimate of the secondary pressure at the virtual location and $\tilde{v}_{sv,m}(n)$ is an estimate of the mth component of the secondary particle velocity at the virtual location. The total acoustic energy density at the virtual location is then calculated using Eq. 1.

EXPERIMENTAL METHOD

The performance of an active noise control system in generating a localised zone of quiet at a fixed virtual energy density sensor was investigated in real-time experiments. Active noise control was also performed at a virtual microphone to compare the size of the zone of quiet achieved by minimising the acoustic energy density and the squared pressure at a virtual location. In acoustic pressure control, the virtual microphone was generated using the remote microphone technique (Roure and Albarrazin 1999).

Experiments were conducted in the three-dimensional cavity shown in Fig. 3 with dimensions of 1000 mm $\times$ 800 mm $\times$ 890 mm. In the cavity, an electret microphone was mounted to the stepper-motor driven traverse to enable accurate microphone positioning and scanning of the sound field. Prior to active noise control and after convergence of the controller, the sound field was scanned over three horizontal xy planes separated by a distance of 20 mm, as shown in Fig. 4. Each of the horizontal planes measured 120 mm in the x direction and 100 mm in the y direction and contained 143 equally spaced measurement points. The three horizontal measurement planes were located at a height of $z = 0$ mm, corresponding to the height of the sensors and at $z = \pm 20$ mm, corresponding to a height 20 mm above and below the sensors.

The acoustic energy density sensors used in these experiments were based on the acoustic vector sensors developed by Lockwood and Jones (2006). The energy density sensors consisted of an omnidirectional microphone (Knowles EK-3132) and three orthogonally oriented gradient microphones (Knowles NR-3158) collocated on a thin square metal rod as shown in Fig. 5. The energy density sensor head comprised of the four microphones occupied a volume of approximately 2 cm^3. These energy density sensors directly measure the pressure and the three orthogonal components of pressure gradient. To calculate the total instantaneous acoustic energy density in Eq. 1, each of the three orthogonal components of the particle velocity need to be calculated from the corresponding orthogonal components of the pressure gradient. Each of the orthogonal components of particle velocity are related to the corresponding component of pressure gradient through Euler's equation (Nelson and Elliott 1992) by

$$v_{a,m}(n) = \frac{-1}{\rho}\int g_{a,m}(n)dn, \quad (13)$$

where $g_{a,m}(n)$ is the mth component of the pressure gradient. As suggested by Park and Sommerfeldt (1997), the integration required in Eq. 13 can be performed using a digital integrator such that the velocity estimate is calculated using the following recursive formula

$$\tilde{v}_{a,m}(n) = \tilde{v}_{a,m}(n-1) - \frac{g_{a,m}(n)}{\rho f_s} exp\left(\frac{-1}{fs}\right), \quad (14)$$

where f_s is the sampling frequency.

The remote energy density sensing technique uses the error signal from a remotely located energy density sensor to obtain an estimate of the acoustic energy density at the fixed virtual location. In experiments, the physical acoustic energy density sensor was located 50 mm in the x direction from the virtual location. The remote energy density technique requires that a second acoustic energy density sensor be located at the virtual location during the preliminary identification stage. Once the preliminary identification stage is complete, the energy density sensor at the virtual location is removed. In acoustic pressure control, the physical microphone was similarly located 50 mm from the virtual location in the x direction. To obtain an estimate of the acoustic pressure at the virtual location, the remote microphone technique also requires a second microphone be placed at the virtual location during the preliminary identification stage. This microphone is removed once the preliminary identification stage is complete. The acoustic energy density

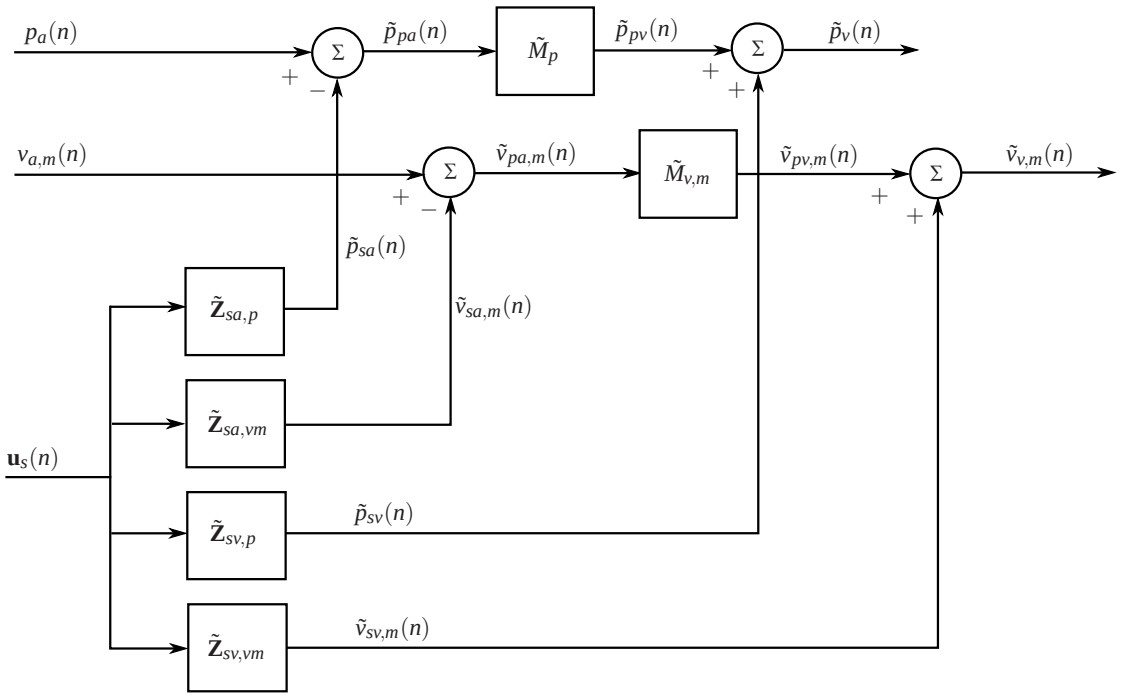

Figure 2: Block diagram of the remote energy density sensing technique. The total acoustic energy density at the virtual location is then calculated using Eq. 1.

Figure 3: The cavity.

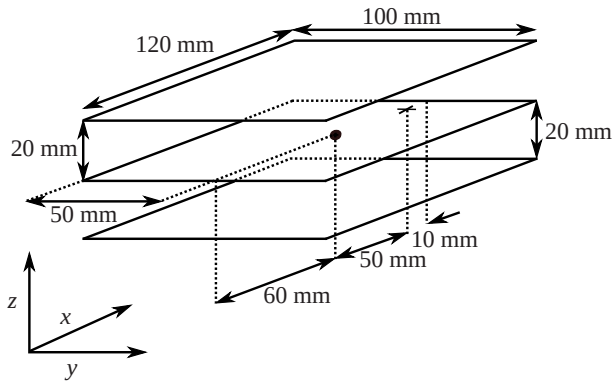

Figure 4: The three horizontal measurement planes. The solid round marker indicates the position of the virtual sensor while the cross indicates the position of the physical sensor. The pitch of the measurement points was 10 mm.

sensors and the microphones were connected to a power supply and an amplifier. The amplified error signals were then sent through a 16-bit PCI-DAS1602/16 multifunction analog and digital I/O Board from Measurement Computing, which was used as a 16-channel AD-converter.

Five 4" loudspeakers were located in the corners of the three-dimensional cavity, one to generate the tonal primary sound field and the other four to act as the secondary sources in acoustic energy density control. The virtual acoustic energy density sensor estimates the acoustic sound pressure and the three orthogonal components of the pressure gradient at the virtual location. As these are four independent quantities, four secondary sources are required to drive the acoustic energy density to zero. If only a single secondary source is used per energy density sensor there will be a trade off between the attenuation achieved at the error sensor location and the size of the localised zone of quiet. The loudspeakers were each excited by control signals which were first passed through a 16-bit PCI-DDA08/16 analog output board from Measurement Computing. This output board was used as an 8-channel DA-converter and an amplifier.

The performance of the virtual energy density algorithm was investigated at the off resonant excitation frequency of 538 Hz. At this frequency, the modal overlap is $M > 4$ illustrating that the sound field is modally dense, as a modal overlap of $M = 3$ defines the boundary between low and high modal density (Nelson and Elliott, 1992). Off resonance excitation of a modally dense sound field results in a number of residual modes contributing to the cavity response and represents the situation most commonly found in practice. In acoustic energy density control, the control signal that drives the secondary loudspeakers, $\mathbf{u}_s(n)$, was calculated using a modified version of the filtered-x LMS algorithm for energy density sensing (Moreau 2010). In acoustic pressure control, only one secondary source is required to minimise the acoustic pressure at the virtual location. The control signal that drives the single secondary loudspeaker, $u_s(n)$, was calculated using the filtered-x LMS algorithm (Nelson and Elliott 1992). In both acoustic

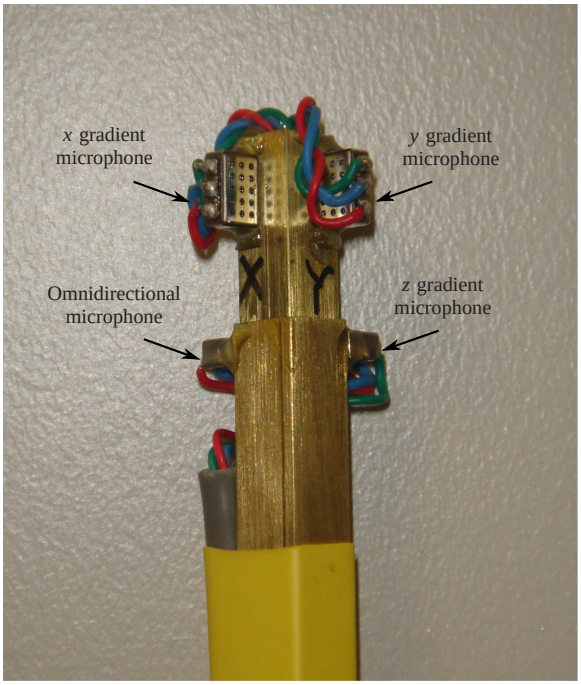

Figure 5: The acoustic energy density sensor consisting of an omnidirectional microphone and three orthogonally orientated pressure gradient microphones collocated on a thin metal rod.

energy density and pressure control, the virtual sensing algorithms and the filtered-x LMS algorithms were implemented in real-time using xPC Target (Mathworks 2007a;b).

RESULTS

Contour plots of the attenuation achieved in acoustic energy density control and acoustic pressure control at the virtual location are shown in Figs. 6 and 7. In these figures, contours have been plotted at increments of 1 dB and labelled every 10 dB. Additionally, the 10 dB zone of quiet is indicated with a black dotted line. The attenuation achieved with the two control schemes over the horizontal plane at $z = 20$ mm, corresponding to a height 20 mm above the sensors, is shown in Figs. 6 (a) and 7 (a). Figs. 6 (b) and 7 (b) shows the attenuation achieved in acoustic energy density and pressure control over the horizontal plane at $z = 0$ mm, corresponding to the height of the sensors. In these figures, the virtual sensor location is indicated by the solid round marker while the cross indicates the position of the physical sensor. Figs. 6 (c) and 7 (c) shows the attenuation achieved with the two control schemes over the horizontal plane at $z = -20$ mm, corresponding to a height 20 mm directly below the sensors.

Fig. 6 shows the control performance in the sound field when the acoustic energy density is minimised at the virtual location with four secondary sources. In the $z = 0$ plane, the location of maximum attenuation is centered on the virtual location with 24 dB of attenuation being achieved at this position, as shown in Fig. 6 (b). The 10 dB zone of quiet is approximately oval in shape with a diameter of 60 mm (0.09λ) in the x direction and a diameter of 40 mm (0.06λ) in the y direction. In the $z = 20$ mm plane, the 10 dB zone of quiet is reduced to a size of approximately 30 mm in x direction and 35 mm in the y direction and the maximum attenuation achieved is 20 dB, as shown in Fig. 6 (a). Due to the modal distribution of the sound field, the 10 dB zone of quiet and the location of maximum attenuation have been shifted approximately 10 mm in the x and y directions from the x and y positions of the virtual location, which has a position of $x = 0$, $y = 0$, $z = 0$. In the horizontal plane 20 mm below the plane of the sensors, the 10 dB zone of quiet extends approximately 30 mm in both the x and y directions, as shown in Fig. 6 (c). Again the 10 dB zone of quiet and the location of maximum attenuation have been shifted from the x and y positions of the virtual location to be a distance of 10 mm away in the x direction and 20 mm away in the y direction. The maximum level of attenuation generated in the $z = -20$ mm plane is 15 dB.

The control performance achieved at the virtual location with acoustic pressure control is shown in Fig. 7. Comparing Figs. 6 and 7 shows that increased control performance is achieved in the sound field when the acoustic energy density is minimised at the virtual location with four secondary sources compared to minimising the virtual pressure with a single secondary source. In the $z = 0$ plane, virtual pressure control generates a maximum attenuation of 21 dB at the virtual location and a 10 dB zone of quiet that extends approximately 60 mm (0.06λ) in the x direction and 20 mm (0.03λ) in the y direction, as shown in Fig. 7 (b). Compared to virtual acoustic energy density control, this is a 3 dB reduction in the maximum attenuation achieved at the virtual location. The 10 dB zone of quiet has also been reduced by 20 mm in the y direction. In the $z = 20$ mm plane, virtual acoustic pressure control generates a 10 dB zone of quiet that extends approximately 15 mm in the x direction and 9 mm in the y direction, as shown in Fig. 7 (a). The maximum attenuation level measured in the $z = 20$ mm plane is 10 dB. In comparison to the control performance achieved in the $z = 20$ mm plane with virtual acoustic energy density control, the maximum level of attenuation is reduced by 10 dB with virtual pressure control. The 10 dB zone of quiet is also reduced in size by 15 mm in the x direction and 26 mm in the y direction. In the $z = -20$ mm plane, minimising the acoustic pressure at the virtual location generates a maximum attenuation level of 15 dB and a 10 dB zone of quiet that extends 23 mm in both the x and y directions, as shown in Fig. 7 (c). While the maximum level of attenuation is the same in this plane for both control strategies, acoustic energy density control generates a 10 dB zone of quiet that extends 7 mm further in both the x and y directions. As seen in acoustic energy density control, the 10 dB zone of quiet generated in acoustic pressure control has also been shifted slightly in the x and y directions from the x and y positions of the virtual location in both the $z = 20$ mm and the $z = -20$ mm planes.

CONCLUSION

In this paper, a fixed virtual acoustic energy density method has been presented for use in a three-dimensional sound field. The virtual energy density algorithm creates a spatially extended zone of quiet at a fixed virtual location using a modified version of the remote microphone technique. Real-time experimental results of active noise control in a modally dense three-dimensional sound field demonstrated that minimising the virtual acoustic energy density with four secondary sources provides improved attenuation and a larger 10 dB zone of quiet at the virtual location than virtual microphones and a single secondary source.

While the zone of quiet generated at the fixed virtual energy density sensor is noticeably larger than that generated at a virtual microphone, it is still limited in size. Only when the movement of the virtual location is restricted to a very small region within the sound field would a fixed virtual energy density sensor be a comparable alternative to a moving virtual microphone. A possible extension to this study could be the development of a moving virtual acoustic energy density sensor. Although active noise control at a moving virtual acoustic energy density sensor would not provide any significant increase to the level of attenuation achieved at the virtual location with a moving

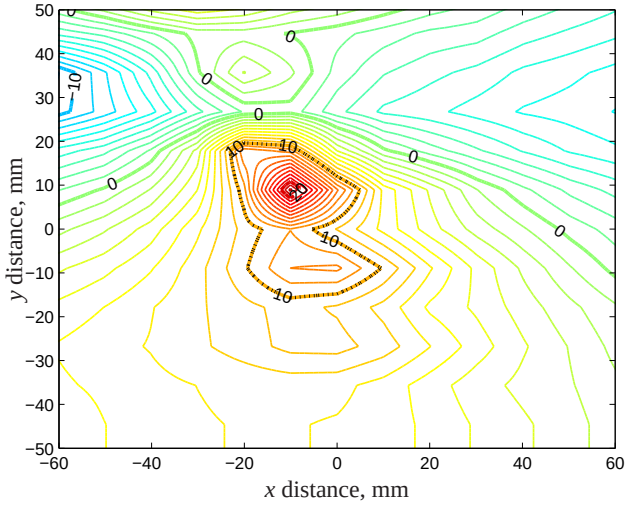

(a) $z = 20$ mm.

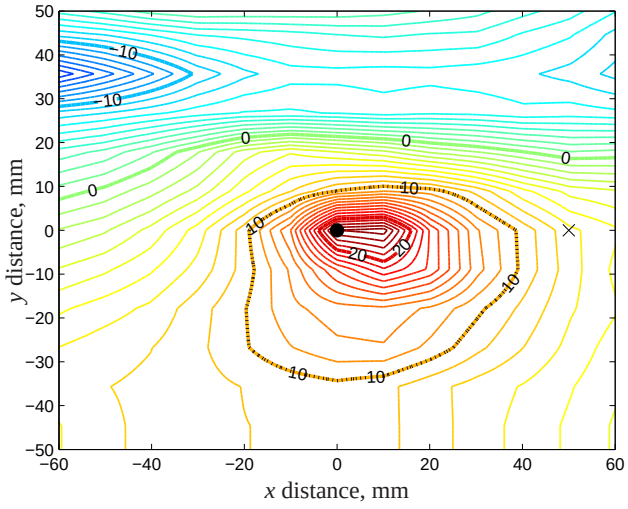

(b) $z = 0$ mm.

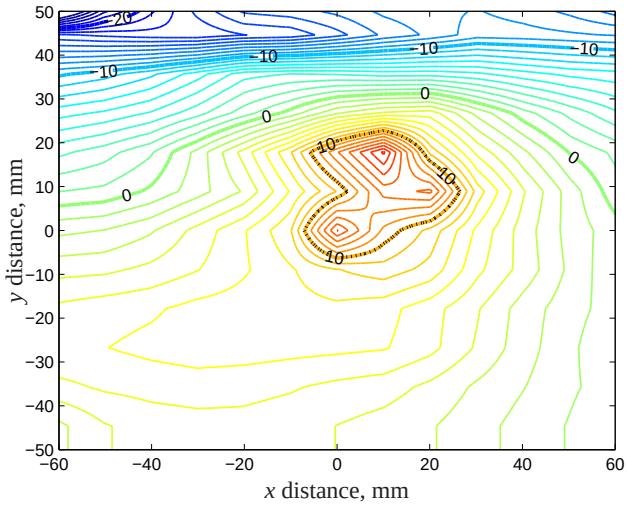

(c) $z = -20$ mm.

Figure 6: Contour plot of the attenuation in dB achieved in acoustic energy density control at the virtual location with four secondary sources. The virtual energy density sensor location is indicated by the solid round marker while the cross indicates the position of the physical energy density sensor.

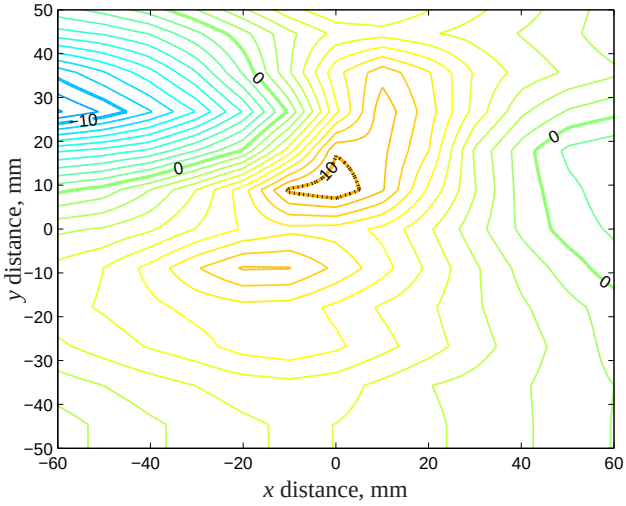

(a) $z = 20$ mm.

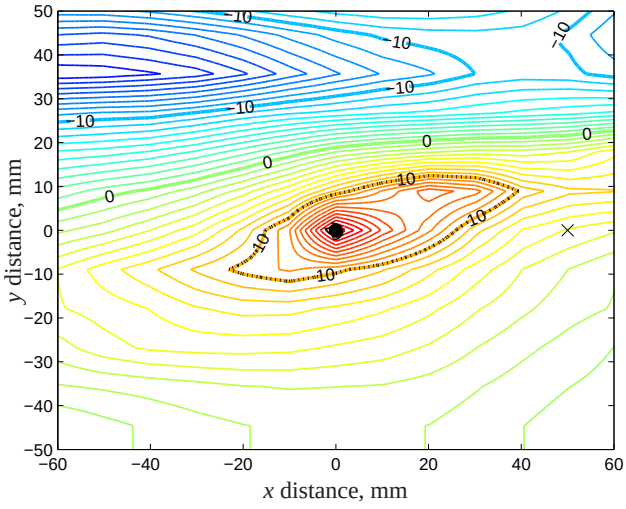

(b) $z = 0$ mm.

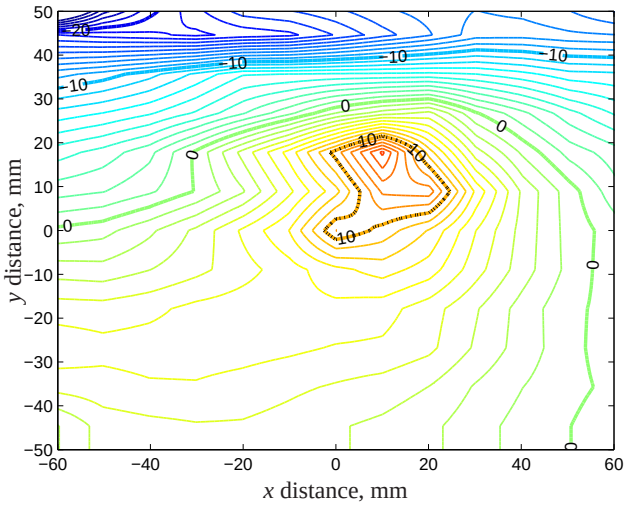

(c) $z = -20$ mm.

Figure 7: Contour plot of the attenuation in dB achieved in acoustic pressure control at the virtual location with a single secondary source. The virtual microphone location is indicated by the solid round marker while the cross indicates the position of the physical microphone.

virtual microphone, it would allow for much slower tracking of the adaptive feedforward control algorithm. The spatial variance of an acoustic energy density cost function is significantly less than that of squared pressure (Sommerfeldt et al. 1995) so the control filter coefficients would not need to be updated as quickly as required in acoustic pressure control.

On a final note, it is also worth considering whether there is any advantage to using a three-dimensional acoustic energy density sensor to four closely spaced microphones arranged to span the three Cartesian axes in active noise control. It has been shown in previous studies that minimising the one-dimensional acoustic energy density at a point or the pressures at two closely spaced locations with two secondary sources results in the same sized zone of quiet at the sensor locations (Elliott and Garcia-Bonito 1995, Moreau et al. 2009b). The advantage in minimising the acoustic energy density lies with observability problems that may arise when measuring the acoustic pressure at discrete locations. Placing the pressure microphones near the pressure nodes of an acoustic mode means that the mode cannot be sensed by the active noise control system and that it may be excited to high amplitudes during control. This does not occur, however, when sensing the acoustic energy density as the velocity amplitude is large at a pressure node and therefore the mode can be sensed by the active noise control system (Sommerfeldt and Nashif 1994).

REFERENCES

B.S. Cazzolato. *Sensing systems for active control of sound transmission into cavities*. PhD thesis, Department of Mechanical Engineering, The University of Adelaide, Australia, 1999.

B.S. Cazzolato. An adaptive LMS virtual microphone. In *Proceedings of Active 2002*, pages 105–116, ISVR, Southampton, UK, 2002.

S.J. Elliott and A. David. A virtual microphone arrangement for local active sound control. In *Proceedings of the 1st International Conference on Motion and Vibration Control*, pages 1027–1031, Yokohama, 1992.

S.J. Elliott and J. Garcia-Bonito. Active cancellation of pressure and pressure gradient in a diffuse sound field. *J. Sound Vib*, 186(4):696–704, 1995.

S.J. Elliott, P. Joseph, A.J. Bullmore, and P.A. Nelson. Active cancellation at a point in a pure tone diffuse sound field. *J. Sound Vib*, 120(1):183–189, 1988.

C. D. Kestell, B. S. Cazzolato, and C. H. Hansen. Virtual sensors in active noise control. *Acoustics Australia*, 29(2):57–61, 2001a.

C.D. Kestell. *Active control of sound in a small single engine aircraft cabin with virtual error sensors*. PhD thesis, Department of Mechanical Engineering, The University of Adelaide, Australia, 2000.

C.D. Kestell, B.S. Cazzolato, and C.H. Hansen. Active noise control with virtual sensors in a long narrow duct. *International Journal of Acoustics and Vibration*, 5(2):63–76, 2000.

C.D. Kestell, B.S. Cazzolato, and C.H. Hansen. Active noise control in a free field with virtual sensors. *J. Acoust. Soc. Am.*, 109(1):232–243, 2001b.

M.E. Lockwood and D.L. Jones. Beamformer performance with acoustic velocity sensors in air. *J. Acoust. Soc. Am.*, 119(1):608–619, 2006.

Mathworks. *Getting Started with xPC Target*. The Mathworks, Inc., Natick, MA, 2007a.

Mathworks. *xPC Target User's Guide*. The Mathworks, Inc., Natick, MA, 2007b.

D.J. Moreau. *Spatially fixed and moving virtual sensing methods for active noise control*. PhD thesis, School of Mechanical Engineering, The University of Adelaide, 2010.

D.J. Moreau, B.S. Cazzolato, and A.C. Zander. Active noise control at a moving virtual microphone using the SOTDF moving virtual sensing method. In *Acoustics 2009*, Adelaide, Australia, 2009a.

D.J. Moreau, J. Ghan, B.S. Cazzolato, and A.C. Zander. Active noise control in a pure tone diffuse sound field using virtual sensing. *J. Acoust. Soc. Am.*, 125(6):3742–3755, 2009b.

P.A. Nelson and S.J. Elliott. *Active Control of Sound*. Academic Press, 1st edition edition, 1992.

Y.C. Park and S.D. Sommerfeldt. Global attenuation of broadband noise fields using energy density control. *J. Acoust. Soc. Am.*, 101(1):350–359, 1997.

C. D. Petersen, A. C. Zander, B. S. Cazzolato, and C. H. Hansen. Optimal virtual sensing for active noise control in a rigid-walled acoustic duct. *Journal of the Acoustical Society of America*, 118(5):3086–3093, 2005.

C.D. Petersen. *Optimal spatially fixed and moving virtual sensing algorithms for local active noise control*. PhD thesis, School of Mechanical Engineering, The University of Adelaide, Australia, 2007.

C.D. Petersen, B.S. Cazzolato, A.C. Zander, and C.H. Hansen. Active noise control at a moving location using virtual sensing. In *Proceedings of the 13th International Congress on Sound and Vibration*, Vienna, 2006.

C.D. Petersen, R. Fraanje, B.S. Cazzolato, A.C. Zander, and C.H. Hansen. A Kalman filter approach to virtual sensing for active noise control. *Mechanical Systems and Signal Processing*, 22(2):490–508, 2008.

A. Roure and A. Albarrazin. The remote microphone technique for active noise control. In *Proceedings of Active 1999*, pages 1233–1244, Florida, USA, 1999.

S. D. Sommerfeldt and P. J. Nashif. An adaptive filtered-x algorithm for energy based active control. *Journal of the Acoustical Society of America*, 96(1):300–305, 1994.

S.D. Sommerfeldt, J.W. Parkins, and Y.C. Park. Global active noise control in rectangular enclosures. In *Proceedings of Active 1995*, pages 477–488, CA, USA, 1995.